

Astrophysical jets

Gabriela S. Vila

*Instituto Argentino de Radioastronomía (IAR - CONICET)
C. C. N° 5 (1894), Villa Elisa, Buenos Aires, Argentina*

Abstract. The production of jets is a characteristic common to different astrophysical accreting objects at all scales, from long gamma-ray bursts to galactic binaries. Aside from certain phenomenology specific to each type of source, the physical processes underlying the formation and propagation of the jets is believed to be the same. I present some general ideas on the dynamics and energetics of relativistic jets, discussing the mechanisms of ejection, acceleration, and collimation of the outflows. I also focus on the radiative aspects of jets, reviewing the most relevant mechanisms of non-thermal emission with special emphasis in the high-energy regime.

Keywords: Accretion; ISM: jets and outflows; Galaxies: jets; Radiation mechanisms: non-thermal; Gamma rays: general; X-rays: binaries

PACS: 98.62.Nx 98.70.Rz 95.30.Gv 97.80.Jp

INTRODUCTION

Astrophysical jets are collimated, bipolar outflows ejected from the vicinities of a rotating object, that propagate for large distances compared to the size of the launching region.

Systems of very different nature produce jets [1]: supermassive black holes in active galactic nuclei (AGN), stellar-mass black holes or neutron stars in microquasars, young stellar objects (YSOs), and collapsing stars associated to long gamma-ray bursts (GRBs). These sources are among the most powerful in the Universe. The typical power of jets ranges from $\sim 10^{37}$ erg s $^{-1}$ in YSO and microquasars, to $\sim 10^{42} - 10^{47}$ erg s $^{-1}$ in AGN, up to 10^{50} erg s $^{-1}$ in GRBs. Jets in YSOs have bulk velocities of $\sim 10^2 - 10^3$ km s $^{-1}$; these are slow, non-relativistic jets. Relativistic jets can reach velocities close to the speed of light, with bulk Lorentz factors from a few in microquasars, up to $\sim 10^2 - 10^3$ in GRBs.

The phenomenology associated to astrophysical jets is extremely rich. Its study comprises many areas of Physics, from magnetohydrodynamics (MHD) to elementary particle interactions. In this article I present a short review on the dynamical and radiative aspects of astrophysical jets. I begin by introducing, very briefly, the basic concepts of the models for the launching, collimation, and acceleration of jets. Then I discuss in greater detail which are the most relevant radiative processes that contribute to the observed spectrum of jets. Finally, I close by showing some results for the radiation of jets in microquasars obtained with a model developed as part of my research program.

DYNAMICS OF RELATIVISTIC JETS

All sources with relativistic jets have two components in common: a rotating accreting object and an accretion disk. A third fundamental ingredient to launch jets, at least required by most of the models, is a large scale magnetic field.

Two well-established models to explain the launching of jets are the Blandford-Znajek [2] and the Blandford-Payne [3] mechanisms.

The Blandford-Znajek mechanism is a way of extracting energy and angular momentum from a rotating black hole, and transfer them to the electromagnetic field in its surroundings. Since astrophysical black holes are not expected to be charged, the magnetosphere is created by electric currents in the accretion disk.

Blandford and Znajek found a solution for the equations that describe a force-free plasma around a slowly rotating ($a \ll 1$) Kerr black hole immersed in a split monopole magnetic field. An order of magnitude estimate of the total power that can be extracted from the black hole through this process is (see e.g. Ref. [4])

$$L_{\text{BZ}} \approx 10^{45} a^2 \left(\frac{M_{\text{BH}}}{10^9 M_{\odot}} \right)^2 \left(\frac{B_0}{10^4 \text{G}} \right)^2 \text{ erg s}^{-1}, \quad (1)$$

where M_{\odot} is the solar mass, B_0 is the magnetic field strength on the horizon, and a and M_{BH} are the spin and the mass of the black hole, respectively. This power is, in principle, enough to drive the jets in AGN.

The efficiency of the Blandford-Znajek mechanism to produce jets is closely related to the configuration of the black hole magnetosphere and the value of the spin, see for example the discussion in Ref. [5] and references therein. The main results can be summarized as follows. Black hole magnetospheres may be *open* or *closed*, depending on whether open magnetic field lines cross the horizon or not. Closed field lines transfer angular momentum from the black hole to the accretion disk, whereas open lines can transport it to infinity as a jet. The key parameter that determines the configuration of the field lines appears to be the black hole spin. Retrograde¹ ($a < 0$) and rapid prograde ($0.75 < a < 0.99$) black holes are more likely to have open magnetospheres, and then to drive jets. Furthermore, the spin determines the jet power: the most powerful jets are launched from retrograde black holes.

As mentioned in Ref. [5], the above results agree with observations for those AGN with measured spin and jet power. In microquasars, the role of the black hole in the launching of the jets is not clear. Two recent searches for correlations between the jet properties and the spin of the black hole in these sources led to opposite conclusions. No connection was found by Ref. [6], whereas in Ref. [7] the authors claim for a correlation between the spin and the peak radio luminosity at 5 GHz in the case of *discrete* ejections. These studies present two main uncertainties: first, there are only a few stellar-mass black holes with measured spin, and second, the results depend on how the jet power is estimated from the observations. As explained in Refs. [6] and [7], if the Blandford-Znajek or a similar mechanism operates in black holes binaries, it is

¹ A retrograde (prograde) black hole rotates in opposite (same) sense with respect to the accretion disk.

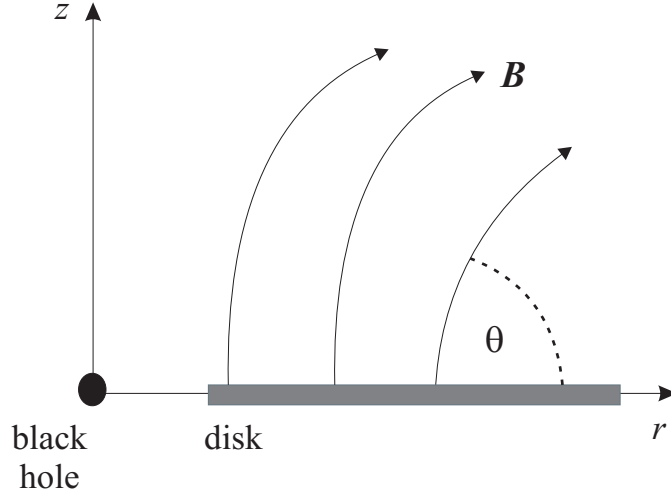


FIGURE 1. Sketch of the poloidal magnetic field lines from the accretion disk. If $\theta < \theta_c$ (see text), the elements of plasma are in unstable equilibrium and accelerate along the field lines.

expected to be responsible for the launching of discrete, and not continuous, outflows. This is because discrete jets are ejected from the immediate surroundings of the black hole (a few $R_{\text{grav}} \equiv GM_{\text{BH}}/c^2$) as the inner radius of the accretion disk approaches the innermost stable orbit, whereas continuous jets form farther away ($\sim 50 - 100 R_{\text{grav}}$) where the relativistic effects are weak.

The Blandford-Payne (or magnetocentrifugal) mechanism of jet launching also relies on the existence of a magnetic field created by the currents in the disk. It is assumed that the footpoints of the field lines are anchored to the disk and get dragged as it rotates. If the inclination of the lines with respect to the outwards radial direction (see Fig. 1) is the appropriate, the plasma is in unstable equilibrium: under perturbations, it becomes accelerated away from the disk along the poloidal field lines. The analogy with beads threaded on a rotating rigid wire is usually employed to describe the movement of the elements of plasma.

As shown, for example, in Ref. [8], in Newtonian or Schwarzschild spacetimes the critical (maximum) inclination angle of the field lines that leads to instability is $\theta_c = 60^\circ$ at any radius.² It is slightly smaller at the innermost stable orbit of a retrograde Kerr black hole with $a = -1$, and approaches $\theta_c = 90^\circ$ for a prograde black hole with $a = 1$. The smaller the value of the critical angle, the less collimated the outflows are at launching. The best-collimated jets might, then, be launched from maximally rotating prograde black holes, where the magnetocentrifugal mechanism can accelerate particles along magnetic field lines almost parallel to the rotation axis.

Magnetocentrifugal forces accelerate the jet up to the Alfvén surface, defined as the surface where the jet bulk velocity equals the Alfvén speed. In this region the magnetic field lines stop co-rotating with the disk and wind up, developing a significant toroidal

² Since the Blandford-Payne mechanism works in Newtonian spacetime, it is a possible process of jet launching in YSOs.

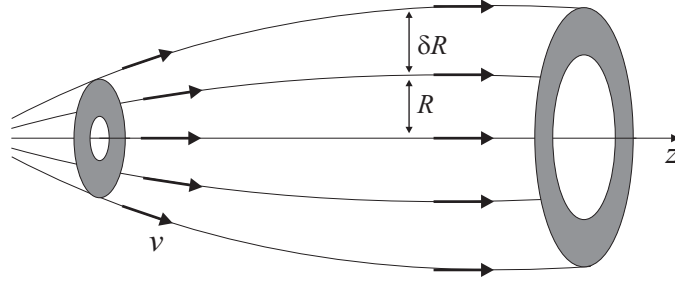


FIGURE 2. Sketch of the flow surfaces in a jet. Adapted from Ref. [10].

component.

Once the jet is launched, its subsequent collimation and acceleration are achieved by the combined action of the magnetic field and the external medium. In the “standard” ideal MHD model of jet dynamics, the outflow accelerates as magnetic energy is converted into bulk kinetic energy. A key parameter of the model is the *magnetization* σ , defined as the ratio of the Poynting flux to the kinetic energy flux across a jet section

$$\sigma = \frac{\text{E.M. energy flux}}{\text{Kinetic energy flux}} \approx \frac{|\mathbf{E} \times \mathbf{B}|}{4\pi\Gamma_{\text{jet}}^2\rho v_p}. \quad (2)$$

where ρ is the mass density and v_p the poloidal velocity of the outflow.

In the launching region the jet is energetically Poynting-dominated, so $\sigma_0 \gg 1$. If the conversion of magnetic into kinetic energy were complete, the maximum Lorentz factor of the jet would be $\Gamma_{\text{jet}}^{\text{max}} = \sigma_0$. MHD acceleration is quite efficient in non-relativistic jets: near the Alfvén surface most of the magnetic energy has converted into kinetic energy and the jet approaches its terminal velocity (see e.g. Ref. [9]). The conversion, however, is not as efficient for relativistic jets.

The efficiency of the acceleration is related to the shape of jet. As explained in Ref. [10], for the bulk Lorentz factor of the jet to increase, the flow surfaces must satisfy a condition of “differential collimation”. If $r(z)$ and $r(z) + \delta r(z)$ are the cylindrical radii of two adjoining flow surfaces (see Fig. 2), then

$$\Gamma_{\text{jet}} \approx \Gamma_{\text{jet}}^{\text{max}} \left(1 - \frac{r}{\delta r} \frac{\delta r_0}{r_0} \right), \quad (3)$$

where r_0 and δr_0 are the initial radius and separation of the surface in question and it was assumed that $\Gamma_{\text{jet}}^0 \ll \Gamma_{\text{jet}}^{\text{max}}$. It is then necessary that the ratio $r/\delta r$ decreases with z for Γ_{jet} to increase. A conical jet, for example, corresponds to $r/\delta r = \text{constant}$ and therefore does not accelerate.

The problem is whether the outflow can attain the condition of differential collimation. It has been shown analytically and through numerical simulations (see e.g. Refs. [11, 12, 13]) that the pressure exerted by the toroidal component of the magnetic field plus the confining pressure of an external medium may have the appropriate collimating effect. The nature of the confining medium depends on the type of source. In long GRBs, the external pressure is naturally provided by the collapsing star. In AGN and microquasars,

the corona or a slow wind expelled from the accretion disk might help confine the jet. This mechanism works as long as the external pressure behaves as $p_{\text{ext}} \propto z^{-\alpha}$, where $\alpha < 2$.³ Such a pressure profile results in a parabolic jet with a Lorentz factor that increases as $\Gamma_{\text{jet}} \propto R_{\text{jet}} \propto z^{\alpha/4}$. Under favorable confining conditions, the model predicts that equipartition ($\sigma \sim 1$) between the magnetic and kinetic energy densities may be reached. Further decrease of the magnetization occurs over very large spatial scales [13], raising the question of whether the conditions of the external medium can remain the appropriate.

Beyond the region where standard MHD acceleration becomes inefficient, other processes may contribute to increase the bulk Lorentz factor of relativistic jets up to the large values inferred specially in AGN and GRBs. Some alternatives are reviewed in Refs. [10] and [5]; these include energy dissipation by magnetic reconnection or magnetic instabilities, recollimation shocks, and impulsive jet ejection. In Refs. [11] and [14] it is shown that in a collapsar the jets can suffer an abrupt re-acceleration when they break the surface of the collapsing star and become deconfined. Time-dependent numerical simulations by these authors yield Lorentz factors $\Gamma_{\text{jet}} \approx 10^2 - 10^3$, in agreement with those inferred for long GRBs.

RADIATION FROM JETS

The radiative spectrum of relativistic jets is non-thermal. It originates in the interaction of relativistic particles in the jets with matter, radiation, and magnetic field. Typically, the spectral energy distribution (SED) of jets is the sum of several contributions in different energy bands and may extend along the whole electromagnetic spectrum, from radio to very high-energy gamma rays.

The presence of relativistic electrons in the jets is clearly revealed by the detection of synchrotron radiation at radio wavelengths (see below). The shape of the synchrotron spectrum indicates that the electrons are distributed in energy following a power-law: $N_e(E) \propto E^{-\beta}$, where N_e is the electron energy distribution (number density per unit energy), and $\beta > 0$ is the spectral index. Some mechanism are known that might accelerate particles in astrophysical environments, for example diffusive shock acceleration (which is also known as first-order Fermi process, see e.g. Refs. [15] and [16]), magnetic reconnection [17, 18], and the converter mechanism [19]. These processes are particularly appealing, since they lead to power-law particle injection functions.

In the diffusive shock acceleration mechanism, particles gain energy as they repeatedly cross a shock front. This is usually claimed to be the acceleration process at work in jets, because internal shocks are expected to develop when regions of the outflow with different velocities collide. The theory of diffusive acceleration in strong (with high Mach number), non-relativistic shocks predicts spectral indices $\alpha = 2.0 - 2.2$ at injection.⁴ Spectral indices $\alpha \sim 1.5$ or harder may arise as a result of diffusive acceleration

³ If, on the contrary, $\alpha > 2$, the jet eventually becomes conical and stops accelerating.

⁴ As discussed later, the power-law index of the particle injection function (α) does not necessarily equal the spectral index of the particle distribution (β), since particles suffer energy losses that modify the

mediated by relativistic shocks [20, 21]. Although these values are in the range inferred from observations, it is not ultimately established that diffusive shock acceleration is the only mechanism that operates in jets. Ideal MHD models predict that the outflows remain Poynting-dominated over very large spatial scales. This condition is unfavorable for particle acceleration through shocks, since for magnetizations $\sigma > 0.1$ the efficiency of shocks to heat the plasma is greatly reduced [22]. The action of other acceleration processes, then, should not be discarded.

The detection of synchrotron emission undoubtedly indicates that there are non-thermal electrons in the jets, but the exact composition of the outflows is uncertain. Jets launched by the Blandford-Znajek mechanism start as a flux of electromagnetic field and get afterwards loaded with electron-positron pairs generated in situ. But if the jets are fed with matter from the accretion disc or the corona, they may also contain baryons. There is evidence of the presence of iron nuclei in one system, the jet of the microquasar SS433 [23]. The presence of relativistic protons in two supernova remnants, Cassiopeia A and Tycho, is deduced from the shape of their high and very high-energy gamma-ray spectrum [24, 25]. Non-thermal particles in supernova remnants are accelerated by the diffusive shock mechanism, so it is reasonable to expect that jets may be populated by very energetic protons and heavier nuclei as well.

The targets with which relativistic particles in the jets interact may be internal or external. The internal targets are the locally generated photon fields, the magnetic field, and the jet's comoving matter field. Different external target fields are relevant depending on the type of source. In AGN, the jets interact with the radiation from the corona and the disk, and the matter in the clouds that orbit the black hole. In microquasars, particularly those with high-mass companion stars, the radiation and the wind of the companion are significant target fields as well. The matter in the interstellar or intergalactic medium also represents a target, specially in the termination region of the jets.

There are a number of radiative processes, involving both relativistic electrons and protons, that may contribute to the SED of jets. I briefly review them below, sorted by the nature of the target field. The reader is referred to Refs. [26, 27] for a more detailed discussion and all the formulas related to the calculation of the cooling rates and luminosities.

- ***Synchrotron radiation.*** This is the most important interaction channel between relativistic particles and the magnetic field in astrophysical jets. The typical synchrotron radio spectrum of jets is approximately flat: the specific flux is well fit by a power-law of the form $S_\nu \propto \nu^\delta$, where $\delta \sim 0$. This spectral shape is consistent with synchrotron radiation from relativistic electrons in an expanding outflow [28], and it is so characteristic that jets are usually discovered through the detection of their radio emission. Synchrotron radio emission has also been detected from the termination regions of jets in YSOs, see e.g. Ref. [29].

The analysis of the synchrotron emission allows to obtain information about the energy distribution of the relativistic particles. If synchrotron radiation is the main cooling channel (as it is often the case for high-energy electrons) and the spectrum is a power-

injection spectrum.

law $S_\nu \propto \nu^\delta$, then $N(E) \propto E^{-(2\delta+1)}$.

Synchrotron radiation is a much more efficient cooling process for light particles. This is because the synchrotron energy loss rate (see e.g. [30]) depends on the mass m of the particle as $(m_e/m)^3$; the energy losses are then $\sim 10^9$ times faster for electrons than for protons. Nevertheless, in regions of high magnetic field, synchrotron radiation of very energetic protons may be relevant as well, as has been shown, for example, in Refs. [31, 32] and Ref. [33] in the context of blazars and microquasars, respectively.

• **Inverse Compton scattering.** Inverse Compton (IC) scattering is an efficient mechanism of high-energy emission in many astrophysical sources. The scattering off electrons is more efficient than scattering off heavy particles, and this process is seldom considered as a cooling channel for protons. For a discussion of the theory of IC scattering, the reader is referred to [30].

Inverse Compton scattering can contribute significantly to the high-energy emission spectrum in microquasars. In those systems with a massive, bright companion, the radiation field of the star is a relevant target for IC scattering off the relativistic electrons in the jets. In microquasars with low-mass, old, dim companions, the target is the internal radiation field of the jet - in general the most important field is the synchrotron field of electrons. When a particle scatters its own radiation field, the process is called *Synchrotron Self Compton* (SSC). Several IC emission models are presented, for example, in Ref. [34, 35] for different dominant internal or external target fields. Depending on the model the IC luminosity at ~ 1 GeV can reach $\sim 10^{35}$ erg s $^{-1}$, see Fig. 3.

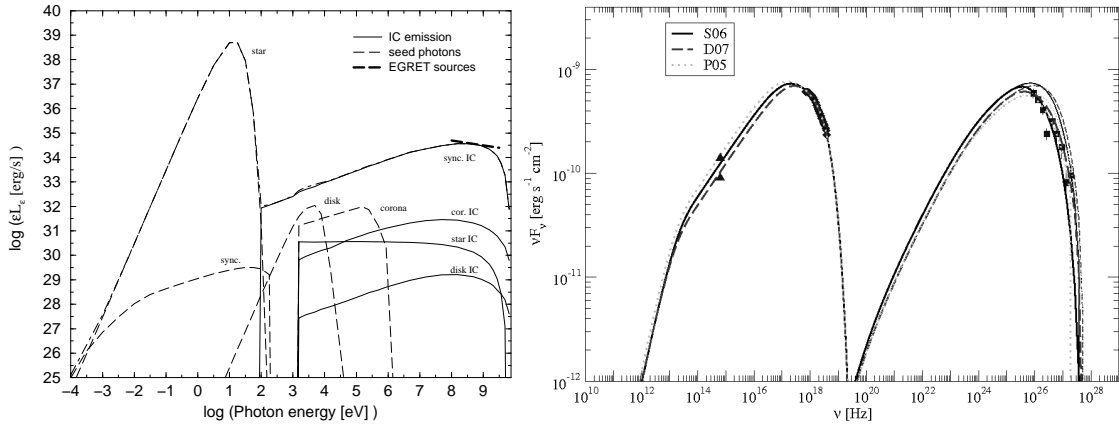


FIGURE 3. Left: SED from a microquasar with a high-mass companion, predicted by the model of Ref. [35]. In this scenario the high-energy emission is due to SSC. The model reproduces the observed spectrum of some EGRET sources. Right: a models for the SED from the 2001 flare of the BL Lac Object Mkn 421. At low energies the emission is produced by synchrotron radiation, and at high energies by Synchrotron Self Compton. From Ref. [36].

IC scattering also contributes to the continuum emission of blazars. The spectrum shows a double-peaked structure: the low-energy peak is due to synchrotron radiation and the high-energy peak due to IC scattering, see Figure 3. The internal low-energy synchrotron photon field is in general the most relevant target and the SSC contribution is the most important one.

• **Photohadronic interactions.** Relativistic protons interact with radiation mainly through direct pair creation

$$p + \gamma \rightarrow p + e^+ + e^-, \quad (4)$$

and pion production

$$p + \gamma \rightarrow p + \pi^0 + a(\pi^+ + \pi^-) \quad p + \gamma \rightarrow n + \pi^+ a\pi^0 + b(\pi^+ + \pi^-). \quad (5)$$

The integers a and b are the pion multiplicities. The decay of neutral pions creates two gamma rays, whereas charged pions decay into muons (which yield electron-positron pairs and neutrinos) and muon neutrinos

$$\pi^0 \rightarrow \gamma + \gamma, \quad (6)$$

$$\pi^+ \rightarrow \mu^+ + \nu_\mu \quad \pi^- \rightarrow \mu^- + \bar{\nu}_\mu, \quad (7)$$

$$\mu^+ \rightarrow e^+ + \nu_e + \bar{\nu}_\mu \quad \mu^- \rightarrow e^- + \bar{\nu}_e + \nu_\mu. \quad (8)$$

Photohadronic interactions might be an important radiative mechanism in sources with high-density photon targets. Ref. [33] presents a model for jets in microquasars with low-mass companion stars that predicts very high-energy electromagnetic emission due to proton-photon collisions. In this model, the synchrotron radiation of relativistic electrons provides a dense target photon field. The gamma-ray emission is produced by the decay of neutral pions and by synchrotron radiation of pairs injected by charged pion decay or direct pair production. Depending on the model parameters, the luminosities corresponding to these processes reach $10^{35-36} \text{ erg s}^{-1}$ above $\sim 1 \text{ TeV}$.

A signature of high-energy proton interactions is the production of neutrinos, injected by the decay of charged mesons and muons. The emission of neutrinos from astrophysical jets has been studied by several authors, see the article by M. Reynoso in these Proceedings for a throughout discussion. In blazars, significant neutrino emission, of the same order of the gamma-ray emission, is predicted for Low-energy cutoff BL Lac objects (LBLs) in the model of Ref. [31], see also Ref. [37]. Neutrino production in microquasars has been considered in Ref. [38]. In this work, it is demonstrated that the energy losses of pions and muons before decay, mainly through synchrotron radiation, may considerably reduce the emissivity of high-energy neutrinos. Neutrino emission from proton-photon collisions is also expected from GRBs, see for example Refs. [39]. Microquasars, AGN, and GRBs are good candidates to be neutrino sources, but up to date the search has yielded negative results (see e.g. [40] for a review of the status of neutrino astronomy). It is expected that the chances of detection improve when the next-generation instruments (KM3NeT and upgrades of IceCube) become available. The detection of neutrinos would definitely prove that protons are accelerated to very high energies in relativistic jets.

- **Proton-proton inelastic collisions.** As proton-photon interactions, the inelastic collision of relativistic protons with low-energy protons creates neutral and charged pions

$$p + p \rightarrow p + p + \pi^0 + a(\pi^+ + \pi^-) \quad p + p \rightarrow p + n + \pi^+ + a\pi^0 + b(\pi^+ + \pi^-). \quad (9)$$

The decay of neutral pions injected in proton-proton collisions may be a relevant mechanism of gamma-ray emission in microquasars with high-mass companion stars and AGN, see Fig. 4.

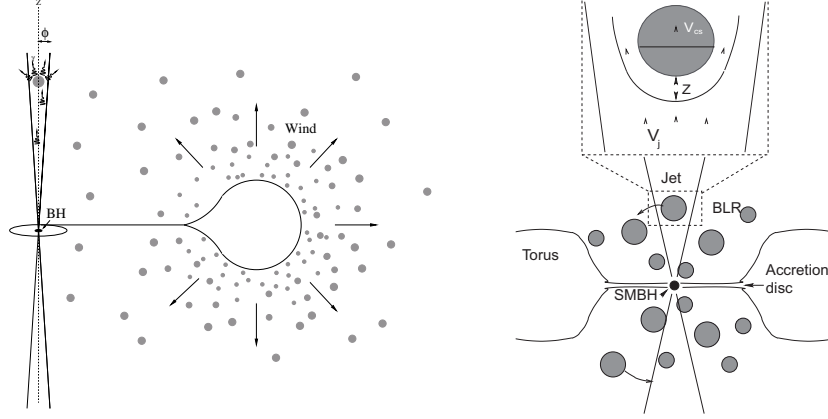


FIGURE 4. Left: sketch of a microquasar with a high-mass, windy donor star. The interaction of the matter in the wind with the relativistic protons in the jets produces gamma rays by decay of neutral pions created in proton-proton inelastic collisions. From Ref. [41]. Right: the interactions of relativistic protons in the jets of an AGN with the clouds of the Broad Line Region, may produce gamma rays by proton-proton collisions, too. From Ref. [42].

In high-mass microquasars, the donor stars have strong winds that serve as a matter target field for the relativistic protons in the jets. As shown in [43] (see also Refs. [44, 45]), detectable gamma-ray luminosities of up to $\sim 10^{35-36}$ erg s $^{-1}$ at $E_\gamma \sim 10$ GeV are obtained by this mechanism. Stellar winds are not homogeneous, but present regions of higher density known as *clumps*. If a clump penetrates the jet, this may produce a high-energy flare because of a sudden increase in the proton-proton collision rate. This scenario has been considered in Refs. [41, 46]. Recently, [47] proposed a model of jet-clump interaction to explain the high-energy flaring emission of the microquasar Cygnus X-1 [48, 49]. These authors estimated that the time for the clump to cross the jet is $\sim 10^4$ s, consistent with the rising time of the 2006 flare observed in this source.

A similar model has been proposed for the high-energy emission from AGN jets. In this case, the protons in the jets interact with the matter in the clouds of the Broad Line Region, see, for example, the works of Ref. [50] and more recently Refs. [42, 51].

- **Relativistic Bremsstrahlung.** Bremsstrahlung radiation is emitted when relativistic electrons are accelerated in the electrostatic field of a nucleus or atom. Bremsstrahlung emission might contribute to the spectrum of sources embedded in high-density environments. In systems with jets, high matter densities are found in the molecular clouds that surround YSOs. As it was shown in Ref. [41] in the case of the YSO IRAS 16547-4227, the density of Hydrogen nuclei in the radio lobes of this source may be as high as

$\sim 2 \times 10^4 \text{ cm}^{-3}$. In these regions, where the jets are halted by the pressure of the matter of the molecular cloud, shock waves may accelerate electrons. According to the results of Ref. [41], Bremsstrahlung emission from these particles might produce gamma rays with energies between $\sim 1 \text{ MeV}$ and $\sim 10 \text{ GeV}$.

A radiative model for jets in low-mass microquasars

We have developed a steady-state jet model for the radiation of microquasars with low-mass companion stars. The model and several applications are presented in Refs. [33, 52, 53, 54].

The basics of the model are the following. We assume that two jets are launched perpendicularly to the accretion disk. The outflows are formed at a distance $z_0 = 50R_{\text{grav}}$ ⁵ from a stellar-mass black hole, and expand as cone as they propagate away from the central engine. Although we do not deal with dynamics of the jets, we assume that they are launched by a magnetocentrifugal mechanism. The jet power in the launching region is basically in the form of magnetic energy; we assume that at large distances from the black hole the magnetic energy has converted almost completely into bulk kinetic energy. This allows us to estimate the magnetic field at z_0 . For a typical jet power $L_{\text{jet}} \sim 10^{36} - 10^{38} \text{ erg s}^{-1}$, we obtain $B(z_0) \sim 10^6 - 10^7 \text{ G}$.

The magnetic field strength decreases with the distance to the compact object. At a certain distance z_{acc} where the magnetic energy density is in sub-equipartition with the kinetic energy density, shock waves develop that accelerate particles through some mechanism we do not specify. Our model is *lepto-hadronic*: we assume that both relativistic electrons and protons are injected. The proton-to-electron power ratio, $a \equiv L_p/L_e$ is a key parameter of the model. We are interested in studying the radiation from proton-dominated jets, so we take $a \geq 1$.

The injection function of relativistic particles is a power-law in energy, $Q \propto E^{-\alpha}$ (in units of $\text{erg s}^{-1} \text{ cm}^{-3}$). After being injected, particles lose energy by interaction with the radiation, matter, and magnetic field in the jet, and eventually with the radiation field from the accretion disk.⁶ We consider all the radiative cooling processes described above (synchrotron radiation, Bremsstrahlung, IC, and proton-proton and proton-photon collisions), as well as adiabatic energy losses. We calculate the steady-state particle energy distributions, $N(E, z)$, solving an adequate version of the transport equation, see for example Ref. [55]. This equation takes into account the effects of cooling, propagation, and escape of particles from the injection region. We consider two different cases: the injection and cooling of particles in a compact, homogeneous, region (*one-zone* approximation), and in a spatially extended, inhomogeneous region.

Once the particle energy distributions are known, it is possible to calculate the spectral energy distribution of the jets. We consider not only the radiative contribution of protons and electrons, but also that of pions, muons, and electron-positron pairs produced in

⁵ The z -axis is the symmetry axis of the jet, see Fig. 2.

⁶ We do not consider the interaction with the wind and radiation from the donor star, that are usually too weak to be relevant targets.

proton-proton and proton-photon collisions, as well as that of pairs created by photon-photon annihilation. The resulting SEDs are complex, and can take very different shapes depending on the values of the model parameters.

Figure 5 shows fits of the radio-to-X-ray data of the low-mass microquasar XTE J1118+480 during outburst in 2000 and 2005, obtained with our model [54]. The observations are well explained as synchrotron radiation from relativistic electrons in the jets (that extends up to the X-rays) plus thermal radiation from the accretion disk. At high energies, there is appreciable emission above 10 GeV due to pion decay created in proton-proton interactions. The results of the model predict that during a future outburst of similar characteristics, this source would be detectable at high and very high-energy gamma rays with available and future instruments, like the satellite *Fermi* and the Cherenkov telescopes MAGIC and CTA.

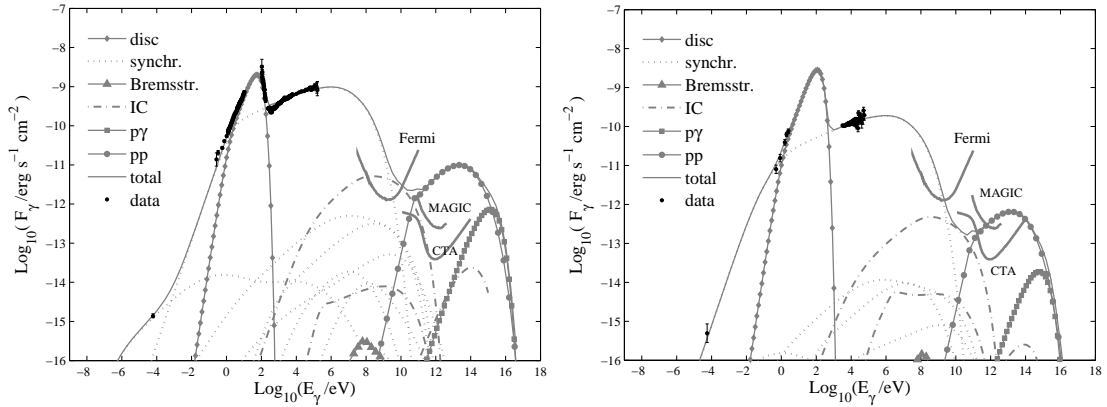


FIGURE 5. Best-fit SEDs of the data taken during the outbursts of 2000 (left) and 2005 (right) of the microquasar XTE J1118+480. From Ref. [54].

Figure 6 shows the best-fit of the observations of the low-mass microquasar GX 339-4 during the outbursts of 1997 and 1999 [53]. Notice that in the best-fit model for the 1997 outburst, there is significant contribution to the SED of synchrotron radiation from protons and secondary particles, especially pions and electron-positron pairs. Our model predicts that the gamma-ray emission of this source during a future outburst may be detectable.

FINAL REMARKS

Our understanding of astrophysical jets has considerably progressed during the last few years. Thanks to theoretical work and huge numerical simulations, the MHD model of jet launching, acceleration, and collimation is well understood. This model can explain many aspects of the dynamics of jets, but there still remain some blanks. New approaches to the problem are being explored, that will hopefully provide satisfactory explanations to the problems of the present models.

There are no available models that fully couple the dynamics and radiation of jets. This a complex problem, that will be for sure tackled in the near future with the help of supercomputers. Detailed predictions, however, can be made for the radiative spectrum

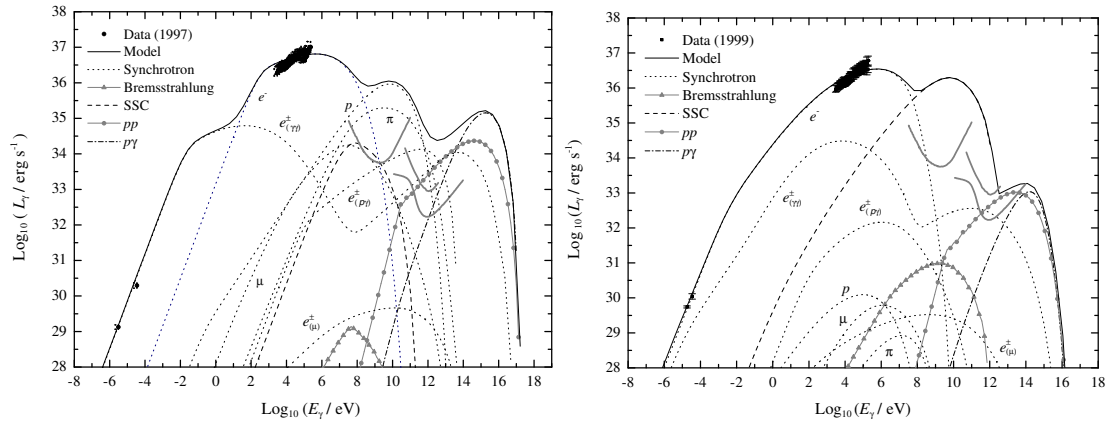


FIGURE 6. Best-fit SEDs of the data taken during the outbursts of 1997 (left) and 1999 (right) of the microquasar GX 339-4. From Ref. [53].

of jets as we have shown. The quality and quantity of the data that may be presently obtained will help to test the predictions of the radiative models. This represents a valuable way of gathering information about the physical conditions in the jets and their surroundings. In particular, observations in the gamma-ray band may provide information about the contents of the outflows and their efficiency to accelerate particles.

ACKNOWLEDGMENTS

I would like to thank the organizers of the First Argentinian-Brazilian Meeting on Gravitation, Astrophysics, and Cosmology for the invitation to present this talk.

REFERENCES

1. G. Romero, R. Sunyaev, and T. Belloni, editors, *Proceedings IAU Symposium No. 275 "Jets at All Scales"*, vol. 6, Cambridge University Press, 2010.
2. R. D. Blandford, and R. L. Znajek, *Mon. Not. R. Astron. Soc.* **179**, 433–456 (1977).
3. R. D. Blandford, and D. G. Payne, *Mon. Not. R. Astron. Soc.* **199**, 883–903 (1982).
4. V. S. Beskin, *MHD Flows in Compact Astrophysical Objects. Accretion, Winds and Jets*, Springer, 2010, first edn.
5. D. L. Meier, “The formation of relativistic cosmic jets,” in *Jets at All Scales*, edited by G. E. Romero, R. A. Sunyaev, & T. Belloni, 2011, vol. 275 of *IAU Symposium*, pp. 13–23.
6. R. P. Fender, E. Gallo, and D. Russell, *Mon. Not. R. Astron. Soc.* **406**, 1425–1434 (2010).
7. R. Narayan, and J. E. McClintock, *Mon. Not. R. Astron. Soc. Lett.* **419**, L69–L73 (2012).
8. M. Lyutikov, *Mon. Not. R. Astron. Soc.* **396**, 1545–1552 (2009).
9. D. Giannios, *Journal of Physics Conference Series* **283**, 012015 (2011).
10. S. S. Komissarov, *Memor. Soc. Astronom. Ital.* **82**, 95–103 (2011).
11. A. Tchekhovskoy, J. C. McKinney, and R. Narayan, *Mon. Not. R. Astron. Soc.* **388**, 551–572 (2008).
12. S. S. Komissarov, N. Vlahakis, A. Königl, and M. V. Barkov, *Mon. Not. R. Astron. Soc.* **394**, 1182–1212 (2009).
13. Y. Lyubarsky, *Astrophys. J.* **698**, 1570 (2009).
14. A. Tchekhovskoy, R. Narayan, and J. C. McKinney, *New Astron.* **15**, 749–754 (2010).
15. A. R. Bell, *Mon. Not. R. Astron. Soc.* **182**, 147 (1978).

16. L. O. Drury, *Reports on Progress in Physics* **46**, 973–1027 (1983).
17. S. Zenitani, and M. Hoshino, *Astrophys. J.* **562**, L63–L66 (2001).
18. G. Kowal, E. M. de Gouveia Dal Pino, and A. Lazarian, *Astrophys. J.* **735**, 102 (2011).
19. E. V. Derishev, F. A. Aharonian, V. V. Kocharovskiy, and V. V. Kocharovskiy, *Phys. Rev. D* **68**, 043003 (2003).
20. F. W. Stecker, M. G. Baring, and E. J. Summerlin, *Astrophys. J. Lett.* **667**, L29–L32 (2007).
21. E. J. Summerlin, and M. G. Baring, *ArXiv e-prints* (2011), 1110 . 5968.
22. C. F. Kennel, and F. V. Coroniti, *Astrophys. J.* **283**, 710–730 (1984).
23. S. Migliari, R. Fender, and M. Méndez, *Science* **297**, 1673–1676 (2002).
24. M. Araya, and W. Cui, *Astrophys. J.* **720**, 20–25 (2010).
25. G. Morlino, and D. Caprioli, *ArXiv e-prints* (2011), 1105 . 6342.
26. G. S. Vila, and F. A. Aharonian, “Radiation processes in high-energy astrophysics,” in *Compact Objects and their Emission*, edited by G. E. Romero, and P. Benaglia, Asociación Argentina de Astronomía, Book Series, Editorial Paideia, La Plata, Argentina, 2009, pp. 1–38.
27. G. E. Romero, and J. M. Paredes, *Introducción a la Astrofísica Relativista*, Publicacions i Edicions de la Universitat de Barcelona, Barcelona, 2011, first edn.
28. R. D. Blandford, and A. Konigl, *Astrophys. J.* **232**, 34–48 (1979).
29. G. Garay, K. J. Brooks, D. Mardones, and R. P. Norris, *Astrophys. J.* **587**, 739–747 (2003).
30. G. R. Blumenthal, and R. J. Gould, *Rev. Mod. Phys.* **42**, 237–271 (1970).
31. A. Mücke, and R. J. Protheroe, *Astroparticle Physics* **15**, 121–136 (2001).
32. F. A. Aharonian, *Mon. Not. R. Astron. Soc.* **332**, 215–230 (2002).
33. G. E. Romero, and G. S. Vila, *Astron. Astroph.* **485**, 623–631 (2008).
34. M. M. Kaufman Bernadó, G. E. Romero, and I. F. Mirabel, *Astron. Astroph.* **385**, L10–L13 (2002).
35. V. Bosch-Ramon, G. E. Romero, and J. M. Paredes, *Astron. Astroph.* **429**, 267–276 (2005).
36. J. D. Finke, C. D. Dermer, and M. Böttcher, *Astrophys. J.* **686**, 181–194 (2008).
37. A. M. Atoyan, and C. D. Dermer, *Astrophys. J.* **586**, 79–96 (2003).
38. M. M. Reynoso, and G. E. Romero, *Astron. Astroph.* **493**, 1–11 (2009).
39. P. Mészáros, and E. Waxman, *Physical Review Letters* **87**, 171102 (2001).
40. A. Kappes, *ArXiv e-prints* (2011), 1110 . 6840.
41. A. T. Araudo, V. Bosch-Ramon, and G. E. Romero, *Astron. Astroph.* **503**, 673–681 (2009).
42. A. T. Araudo, V. Bosch-Ramon, and G. E. Romero, *Astron. Astroph.* **522**, A97 (2010).
43. G. E. Romero, D. F. Torres, M. M. Kaufman Bernadó, and I. F. Mirabel, *Astron. Astroph.* **410**, L1–L4 (2003).
44. G. E. Romero, H. R. Christiansen, and M. Orellana, *Astrophys. J.* **632**, 1093–1098 (2005).
45. M. Orellana, P. Bordas, V. Bosch-Ramon, G. E. Romero, and J. M. Paredes, *Astron. Astroph.* **476**, 9–15 (2007).
46. S. P. Owocki, G. E. Romero, R. H. D. Townsend, and A. T. Araudo, *Astrophys. J.* **696**, 690–693 (2009).
47. G. E. Romero, M. V. Del Valle, and M. Orellana, *Astron. Astroph.* **518**, A12 (2010).
48. J. Albert, and the MAGIC Collaboration, *Astrophys. J. Lett.* **665**, L51–L54 (2007).
49. S. Sabatini, and the AGILE Collaboration, *Astrophys. J. Lett.* **712**, L10–L15 (2010).
50. A. Dar, and A. Laor, *Astrophys. J. Lett.* **478**, L5 (1997).
51. A. T. Araudo, V. Bosch-Ramon, and G. E. Romero, *International Journal of Modern Physics D* **19**, 931–936 (2010).
52. G. E. Romero, and G. S. Vila, *Astron. Astroph.* **494**, L33–L36 (2009).
53. G. S. Vila, and G. E. Romero, *Mon. Not. R. Astron. Soc.* **403**, 1457–1468 (2010).
54. G. S. Vila, G. E. Romero, and N. A. Casco, *ArXiv e-prints* (2011), 1112 . 2560.
55. V. Ginzburg, and S. Syrovatskii, *Origin of Cosmic Rays*, Macmillan, New York, 1964, first edn.